Hindawi
International Journal of Antennas and Propagation
Volume 2019, Article ID 4703161, 7 pages
https://doi.org/10.1155/2019/4703161

Research Article

Flexible Phase Difference of 4 × 4 Butler Matrix without Phase-Shifters and Crossovers

Ke Han, Wuyu Li, and Yibin Liu

School of Electronic Engineering, Beijing University of Posts and Telecommunications, Haidian District, Beijing 100876, China

Correspondence should be addressed to Ke Han; hanke@bupt.edu.cn

Received 21 August 2019; Revised 6 November 2019; Accepted 18 November 2019; Published 4 December 2019

Academic Editor: Atsushi Mase

This paper proposes a new Butler matrix topology. The proposed Butler matrix consists of only four couplers without phase shifters and crossovers. The output phase difference is relatively flexible. Compared with the phase differences (±45° and ±135°) generated by the conventional Butler matrix, the proposed design can generate different sets of phase differences, which can be realized from −180° to 180°. The proposed new Butler matrix replaces the traditional 90° coupler with arbitrary phase-difference couplers. In this paper, closed-form design equations are derived and presented. A 4 × 4 Butler matrix with output phase differences of −30°, +150°, −120°, and +60° is designed according to equations. The 4 × 4 Butler is meant to operate at 2 GHz. The simulation results show that the amplitude unbalance is less than 0.1 dB, the phase mismatch is within 1°, the return loss is higher than 29 dB, and the isolation is higher than 32 dB.

1. Introduction

In recent years, multibeam antennas have been widely used in the military and civilian fields. For example, air/space/ground network, unmanned aerial vehicle (UAV) reconnaissance, and battlefield situation broadcast system all use multibeam antennas. Multibeam antennas can form multiple beams, which make full use of the aperture efficiency of the antenna. Since it can form multiple beams, the area of its feed network is smaller and more compact than a conventional single beam antenna. There are many multibeam antenna feed networks, such as Blass matrix [1], Rotman lens [2], Nolen matrix [3, 4], and Butler matrix [5, 6]. The most famous of these is the Butler matrix due to its simpler topology and low power dissipation [7]. Moreover, by taking advantage of its beam orthogonality, which gives it the capability of transmitting and receiving multiple beams concurrently, its beam scanning coverage and the channel capacity significantly improved [8]. The traditional Butler matrix network is a passive network. By exciting one of the input ports, the equal-amplitude and progressive-phase distribution responses can be generated at the output ports. The traditional 4 × 4 Butler matrix consists of four 90° couplers, two crossovers and two 45° phase shifters. Nowadays, the research on the Butler matrix mostly focuses on flexible output phase difference, wide band engineering, and size reduction. The ultrawideband Butler matrix is realized by using a multilayer structure [9]. By using −45° couplers, a compact Butler matrix can be achieved without phase shifters [10]. A single-layer Butler matrix without phase shifters and crossovers has been proposed [11]. However, its output phase difference is not flexible, only ±45° and ±135°. A flexible output phase difference of Butler matrix topology was established by using couplers with arbitrary phase differences [12]. However, the matrix topology is complex, which is not conducive to integration.

Therefore, a feed network topology with flexible output phase difference is proposed in this paper. The output phase difference is more flexible than the traditional Butler matrix, ranging from $-\pi$ to π. This feature can increase the options of feeding modes for antenna array, extending the range of the radiation beam angles. The new Butler matrix consists of only four couplers, which eliminates phase shifters and crossovers compared with traditional Butler matrices, reducing the area and reducing the power dissipation caused by crossovers and phase shifters. Finally, closed-form design equations are presented, which provides a reference for the design of the special radiation angle Butler matrix and streamlines the design process.

2. Design and Theory

The Butler matrix topology proposed in this paper is shown in Figure 1. It consists of four couplers. The phase difference of coupler 1 is β_1. The phase difference of coupler 2 is β_2. The phase difference of both coupler 3 and coupler 4 is β_3. P1, P2, P3, and P4 are input ports of the Butler matrix, and P5, P6, P7, and P8 are output ports of the Butler matrix.

The coupler used in this Butler matrix is an arbitrary phase-difference hybrid coupler [13]. The coupler is shown in Figure 2. Conventional couplers' output phase difference is 90°. The arbitrary phase-difference hybrid coupler can generate different sets of phase differences, which can be realized from 0° to 180°. The phase responses of the coupler can be expressed by equations (1)–(3) [13].

$$\angle S_{21} - \angle S_{41} = \beta, \tag{1}$$

$$\angle S_{43} - \angle S_{23} = \pi - \beta, \tag{2}$$

$$\angle S_{41} = \angle S_{23}, \tag{3}$$

where β is the output phase difference of the coupler, and the range is 0 to π. The coupler model is shown in Figure 3.

Arbitrary phase-difference hybrid coupler consists of four branch lines. Z_1, Z_2, and Z_3 are characteristic impedance of branch lines. θ_1, θ_2, and θ_3 are electrical lengths of branch lines.

However, the model in [13] ignores the microstrip discontinuity effect. The microstrip discontinuity effects in the design of arbitrary phase-difference hybrid coupler contain bends and T-junctions. With increasing frequency, the parasitic of discontinuities will cause the performance to deviate from the design, such as center frequency shift, mismatch increase, and performance degradation. In [14], the equivalent model of the T-junction is proposed. According to the T-equivalent model, the correction of the operating frequency and S-parameters is achieved by adjusting the characteristic impedance and electrical length of the four branch lines.

According to the relationship between the output phase difference of the coupler, the phase difference relationship between the output port and the input port can be derived. For the convenience of calculation, it is assumed that the phase response of port P5 is α_1 when port P1 is excited, and the phase response of port P5 is α_2 when port P3 is excited. Table 1 shows the phase of ports P5, P6, P7, and P8 when ports P1, P2, P3, and P4 are excited.

From Table 1, the progressive phase of the output port when input from different ports can be obtained. When ports P1, P2, P3, and P4 are respectively excited, the output phase differences $\Delta\theta_1, \Delta\theta_2, \Delta\theta_3$, and $\Delta\theta_4$ can be obtained as

$$\text{for port1} : \Delta\theta_1 = -\beta_1 = \beta_1 - \beta_3 + 2n_1\pi, \tag{4}$$

$$\text{for port2} : \Delta\theta_2 = \pi - \beta_1 = \beta_1 - \beta_3 - \pi + 2n_2\pi, \tag{5}$$

$$\text{for port3} : \Delta\theta_3 = -\beta_2 = \pi + \beta_2 - \beta_3 + 2n_3\pi, \tag{6}$$

$$\text{for port4} : \Delta\theta_4 = \pi - \beta_2 = \beta_2 - \beta_3 + 2n_4\pi, \tag{7}$$

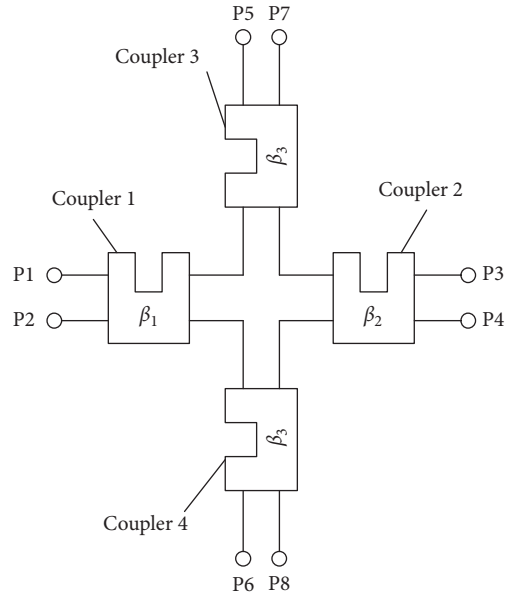

Figure 1: Butler matrix topology.

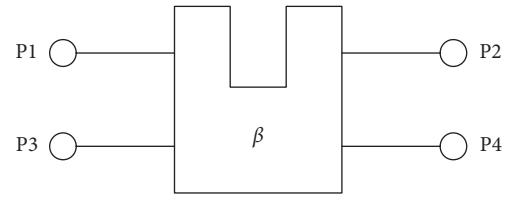

Figure 2: Coupler with β phase difference.

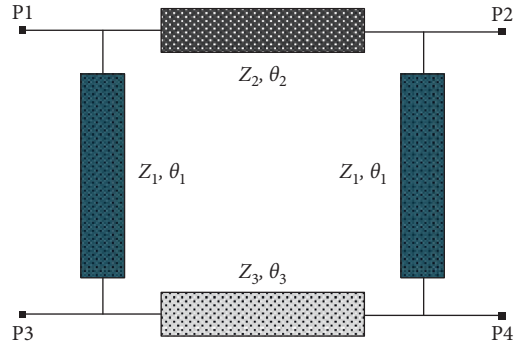

Figure 3: Arbitrary phase-difference hybrid coupler.

Table 1: Phase response of the butler matrix.

Input	Output			
	P5	P6	P7	P8
P1	α_1	$\alpha_1 - \beta_1$	$\alpha_1 - \beta_3$	$\alpha_1 - \beta_1 - \beta_3$
P2	$\alpha_1 - \beta_1$	$\pi + \alpha_1 - 2\beta_1$	$\alpha_1 - \beta_1 - \beta_3$	$\pi + \alpha_1 - 2\beta_1 - \beta_3$
P3	α_2	$\alpha_2 - \beta_2$	$\pi + \alpha_2 - \beta_3$	$\pi + \alpha_2 - \beta_2 - \beta_3$
P4	$\alpha_2 - \beta_2$	$\pi + \alpha_2 - 2\beta_2$	$\pi + \alpha_2 - \beta_2 - \beta_3$	$2\pi + \alpha_2 - 2\beta_2 - \beta_3$

where n_1, n_2, n_3, and n_4 take integers, β_1, β_2, and β_3 take values ranging from 0 to π, and the four output phase differences are not equal ($\Delta\theta_1 \neq \Delta\theta_2 \neq \Delta\theta_3 \neq \Delta\theta_4$). For easy

Table 2: Characteristic impedance and electrical length of the coupler.

Phase difference (°)	Parameter					
	$Z_1(\Omega)$	$Z_2(\Omega)$	$Z_3(\Omega)$	$\theta_1(^\circ)$	$\theta_2(^\circ)$	$\theta_3(^\circ)$
30	25	22.361	22.361	90	127.76	52.24
120	43.301	32.733	32.733	90	69.295	110.705
60	43.301	32.733	32.733	90	110.705	69.295

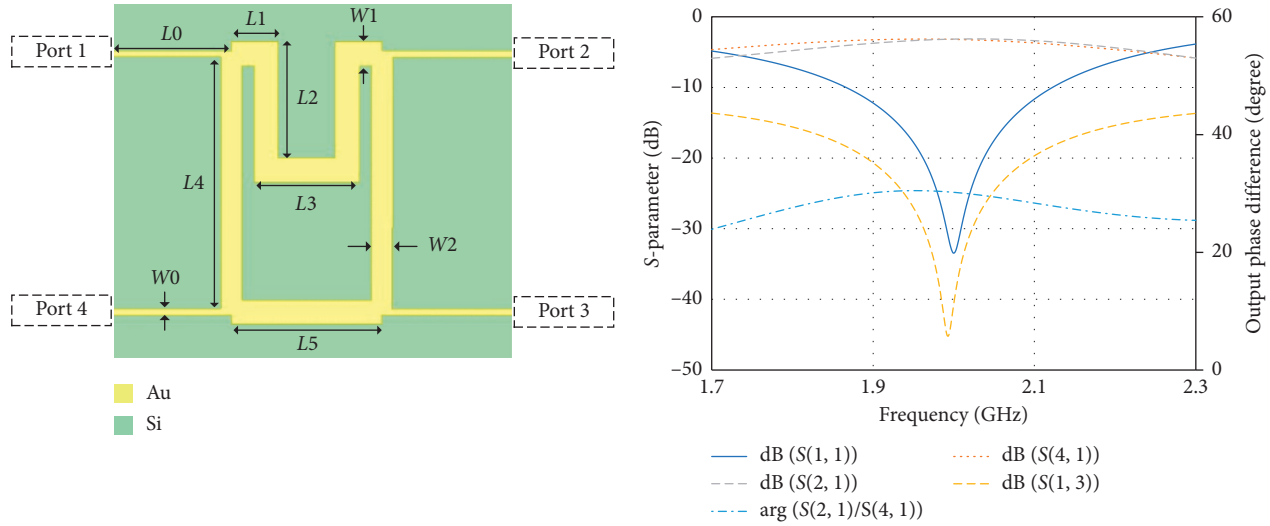

(a) (b)

Figure 4: (a) Coupler model with 30° output phase difference. (b) Simulation of the coupler with 30° output phase difference.

implementation, we set $n_1 = 0$ and $n_3 = 0$. From (4)–(7), the relationship between β_1, β_2, and β_3 can be obtained as

$$\beta_1 = \frac{\beta_3}{2}, \tag{8}$$

$$\beta_2 = \frac{\beta_3}{2} + \frac{\pi}{2}. \tag{9}$$

Substituting (8) and (9) into (4)–(7), the final formulas for the Butler matrix's output phase differences can be derived as

$$\begin{aligned} \Delta\theta_1 &= -\frac{\beta_3}{2}, \\ \Delta\theta_2 &= \pi - \frac{\beta_3}{2}, \\ \Delta\theta_3 &= -\frac{\pi}{2} - \frac{\beta_3}{2}, \\ \Delta\theta_4 &= \frac{\pi}{2} - \frac{\beta_3}{2}. \end{aligned} \tag{10}$$

It can be seen from the above that based on this closed-form design equations, the Butler matrix can be designed according to the required output phase difference, and the output phase difference range can be between $-\pi$ and π. And, the output phase difference is not symmetrical. This feature provides a more flexible choice when feeding the antenna array.

Table 3: Optimized parameters of the coupler.

Parameters	Values (μm)
$L0$	3636
$L1$	1150
$L2$	6197
$L3$	5550
$L4$	13654
$L5$	7850
$W0$	318
$W1$	1281
$W2$	1090

Table 4: Optimized parameters of the coupler.

Parameters	Values (μm)
$L0$	3636
$L1$	2000
$L2$	3704
$L3$	5800
$L4$	14357
$L5$	9800
$W0$	318
$W1$	714
$W2$	430

According to the closed-form design equations, a Butler matrix with output phase differences of −30°, 150°, −120°, and 60° is designed. The phase difference of couplers β_1, β_2,

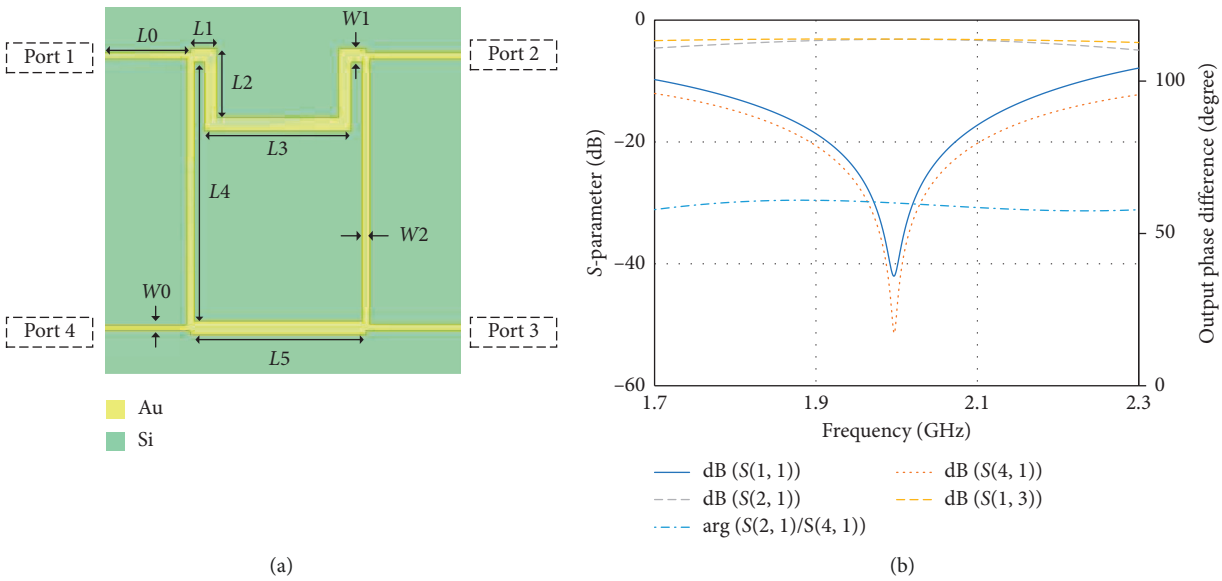

Figure 5: (a) Coupler model with 30° output phase difference. (b) Simulation of the coupler with 30° output phase difference.

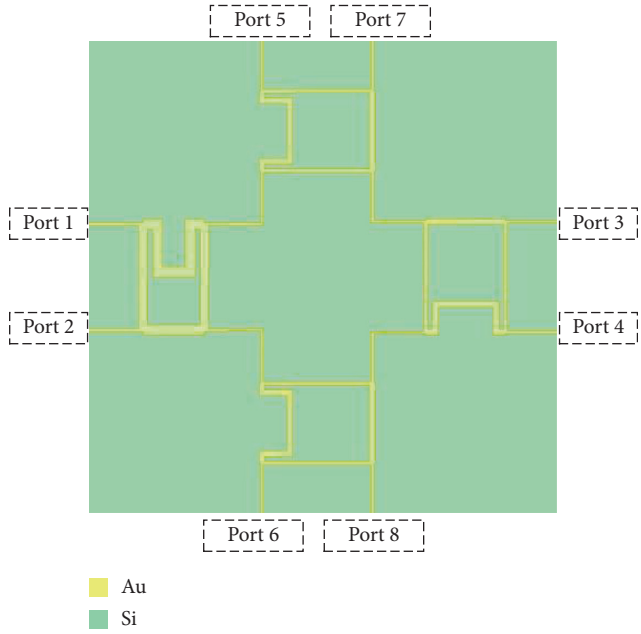

Figure 6: Butler matrix model.

and β_3 in the Butler matrix is 30°, 120°, and 60°, respectively. The characteristic impedance and electrical length parameters of each coupler are shown in Table 2.

3. Simulation

The designed Butler matrix was simulated by HFSS software. The coupler model with 30° output phase difference is shown in Figure 4(a). Table 3 shows the optimized parameters of the coupler. The *S*-parameter showing the reflection coefficient, transmission coefficients and the output phase difference are shown in Figure 4(b). It can be seen from the figure that S_{11} and S_{31} of the coupler are less than −35 dB at 2 GHz. S_{21} and S_{41} are −3.05 dB. The output phase difference is 30.5°.

The coupler with 60° output phase difference and the coupler with 120° output phase difference are symmetrical, so only the coupler with 60° output phase difference is simulated. Table 4 shows the optimized parameters of the coupler. The coupler model with 60° output phase difference is shown in Figure 5(a). The *S*-parameter showing the reflection coefficient, transmission coefficients, and the output phase difference are shown in Figure 5(b). It can be seen from the figure that S_{11} and S_{31} of the coupler are less than −40 dB at 2 GHz. S_{21} and S_{41} are −3.05 dB. The output phase difference is 60.1°.

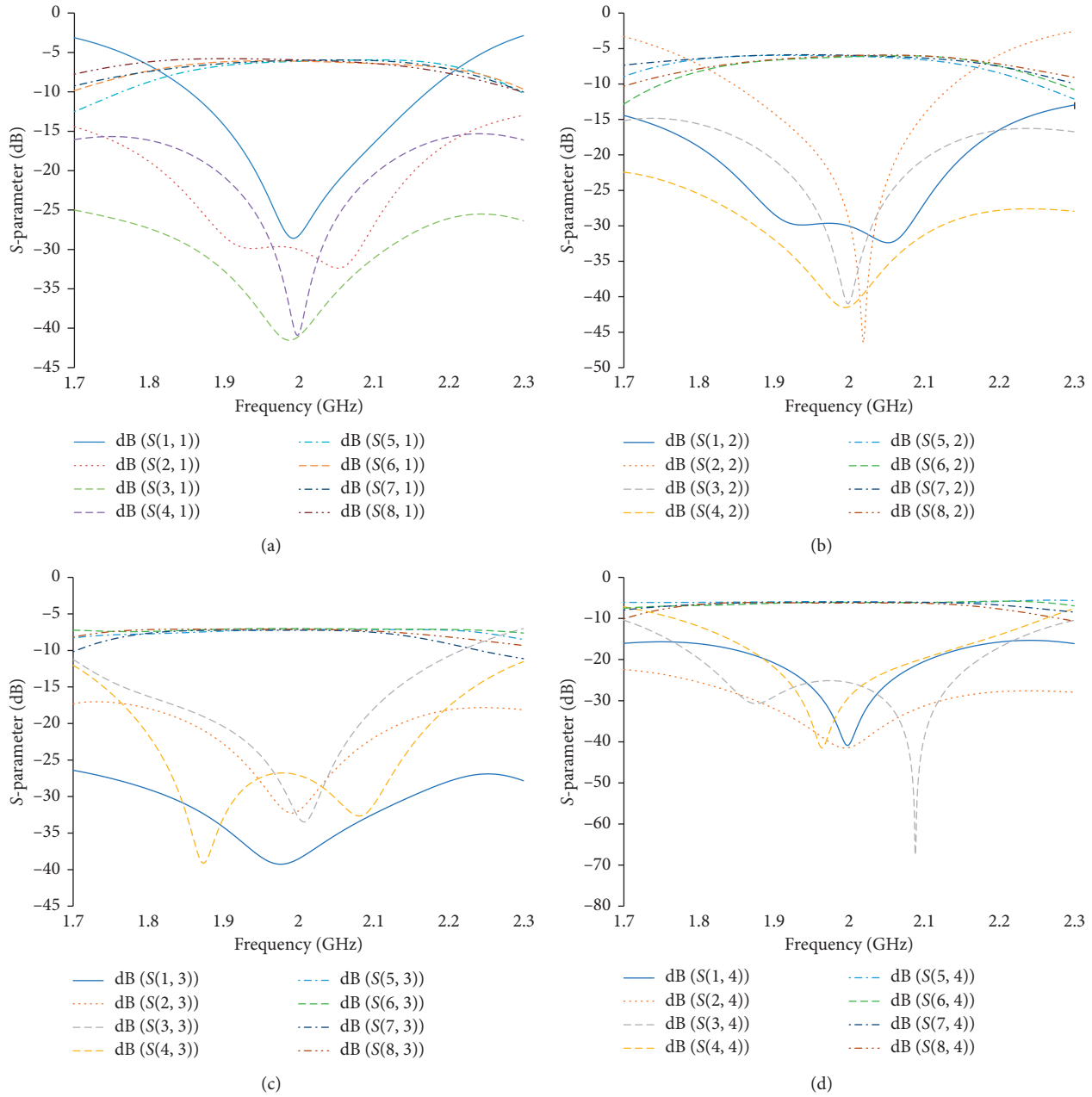

Figure 7: *S*-Parameter of Butler matrix when: (a) port 1 is excited; (b) port 2 is excited; (c) port 3 is excited; (d) port 4 is excited.

The model of the Butler matrix is shown in Figure 6. The *S*-parameter is shown in Figure 7. The output phase difference is shown in Figure 8.

From the simulation results in Figure 7, it can be seen that the signal is input from different ports at 2 GHz, the amplitude imbalance of the output signal is less than 0.1 dB, and the return loss and isolation are both greater than 29 dB. When the signal is input from port 1, its amplitude responses are $S_{51} = -6.07$ dB, $S_{61} = -6.01$ dB, $S_{71} = -6.04$ dB, and $S_{81} = -6.05$ dB. When the signal is input from port 2, its amplitude responses are $S_{52} = -6.02$ dB, $S_{62} = -6.03$ dB, $S_{72} = -6.05$ dB, and $S_{82} = -6.06$ dB. When the signal is input from port 3, its amplitude responses are $S_{53} = -6.05$ dB, $S_{63} = -6.01$ dB, $S_{73} = -6.09$ dB, and $S_{83} = -6.03$ dB. When the signal is input from port 4, its amplitude responses are $S_{54} = -6.01$ dB, $S_{64} = -6.05$ dB, $S_{74} = -6.05$ dB, and $S_{84} = -6.09$ dB.

The differential output phases of the Butler matrix obtained by exciting port 1, port 2, port 3, and port 4 at the center frequency are $-30^{\circ}\pm0.2^{\circ}$, $150^{\circ}\pm1^{\circ}$, $-120^{\circ}\pm0.5^{\circ}$, and $60^{\circ}\pm0.5$, respectively.

Overall, it can be seen that the simulation results of the proposed Butler matrix verify the design concept. The performance of the proposed 4×4 Butler matrix topology is excellent. In contrast to other Butler matrices, it has a flexible output phase difference and reduces size of the topology. In addition, its insertion loss and isolation performance are also excellent. When the Butler matrix is fabricated, the measured results may be worse than the results of the simulation.

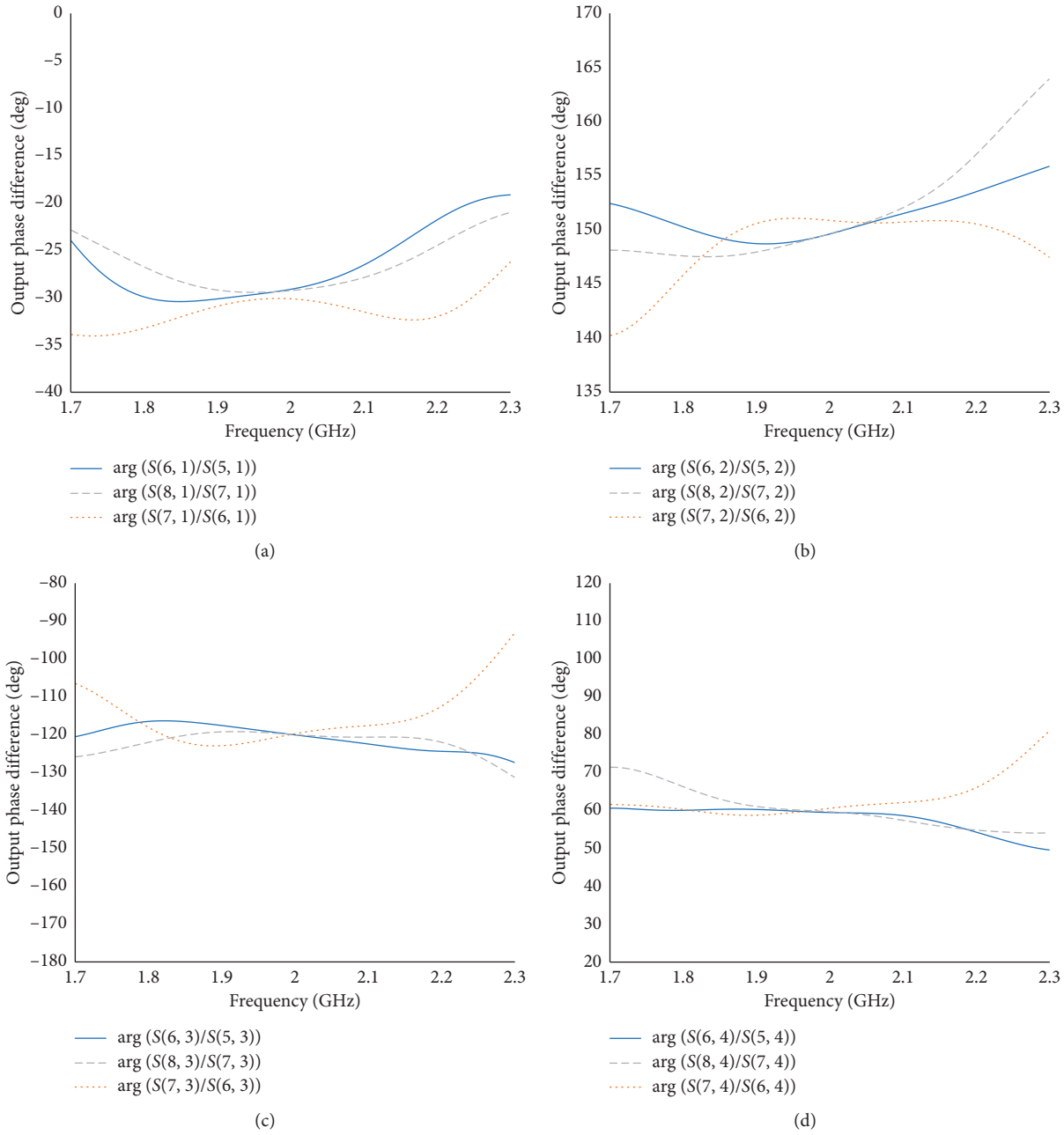

Figure 8: Output phase difference of the Butler matrix when: (a) port 1 is excited; (b) port 2 is excited; (c) port 3 is excited; (d) port 4 is excited.

Due to the impedance mismatch of the port and manufacturing process issues, the insertion loss will increase, and the output phase difference may be slightly offset. But the phase relationship does not change.

4. Conclusion

This paper presents a new 4×4 Butler matrix topology. The proposed Butler matrix consists of only four couplers. A relatively flexible output phase difference can be achieved without the addition of phase shifters and cross couplers. A Butler matrix with phase differences of -30°, $+150^{\circ}$, -120°, and $+60^{\circ}$ is designed. The simulation results at 2 GHz operating frequency show that the amplitude unbalance is less than 0.1 dB, the phase error is within 1°, the return loss is higher than 29 dB, and the isolation is higher than 32 dB. This Butler matrix has excellent performance, and the multibeam antenna based on this feed network can be applied to 5G communication.

Data Availability

The simulation data used to support the findings of this study have been deposited in the Figshare repository (https://figshare.com/articles/butler111_aedt/9703652/1).

Conflicts of Interest

The authors declare that they have no conflicts of interest.

Authors' Contributions

Ke Han and Wuyu Li participated in the design of this study, and they both performed statistical analysis, data acquisition, data analysis, and manuscript preparation. Ke Han carried out data analysis and manuscript preparation. Wuyu Li collected important background information and drafted the manuscript. Yibin Liu provided assistance for data acquisition and manuscript review. Wuyu Li performed literature search and chart drawing. All authors have read and approved the content of the manuscript.

Acknowledgments

This research was supported by the Fundamental Research Funds for the Central Universities (grant no. 2019PTB-016).

References

[1] F. Casini, R. V. Gatti, L. Marcaccioli, and R. Sorrentino, "A novel design method for blass matrix beam-forming networks," in *Proceedings of the 2007 European Microwave Conference*, pp. 1511–1514, IEEE, Munich, Germany, October 2007.

[2] K. Tekkouk, M. Ettorre, L. Le Coq, and R. Sauleau, "Multi-beam SIW slotted waveguide antenna system fed by a compact dual-layer Rotman lens," *IEEE Transactions on Antennas and Propagation*, vol. 64, no. 2, pp. 504–514, 2016.

[3] N. J. G. Fonseca, "Printed S-band 4×4 nolen matrix for multiple beam antenna applications," *IEEE Transactions on Antennas and Propagation*, vol. 57, no. 6, pp. 1673–1678, 2009.

[4] T. Djerafi, N. J. G. Fonseca, and K. Ke Wu, "Planar ku-band 4×4 nolen matrix in SIW technology," *IEEE Transactions on Microwave Theory and Techniques*, vol. 58, no. 2, pp. 259–266, 2010.

[5] S. A. Babale, S. Lawan, S. K. A. Rahim, and I. O. Stella, "Implimentation of 4×4 butler matrix using silver-nono instant inkjet printing technology," in *Proceedings of the 2017 IEEE 3rd International Conference on Electro-Technology for National Development (NIGERCON)*, pp. 514–518, Owerri, Nigeria, November 2017.

[6] J.-W. Lian, Y.-L. Ban, C. Xiao, and Z.-F. Yu, "Compact substrate-integrated 4×8 butler matrix with sidelobe suppression for millimeter-wave multibeam application," *IEEE Antennas and Wireless Propagation Letters*, vol. 17, no. 5, pp. 928–932, 2018.

[7] Y.-S. Lin and J.-H. Lee, "Miniature Butler matrix design using glass-based thinfilm integrated passive device technology for 2.5-GHz applications," *IEEE Transactions on Microwave Theory and Techniques*, vol. 61, no. 7, pp. 2594–2602, 2013.

[8] Q.-L. Yang, Y.-L. Ban, J.-W. Lian, Z.-F. Yu, and B. Wu, "SIW butler matrix with modified hybrid coupler for slot antenna array," *IEEE Access*, vol. 4, pp. 9561–9569, 2016.

[9] A. M. Martir, I. M. Fernandez, and A. O. Monux, "Wideband slotcoupled butler matrix," *IEEE Microwave and Wireless Components Letters*, vol. 24, no. 12, pp. 848–850, 2014.

[10] G. Tian, J.-P. Yang, and W. Wu, "A novel compact Butler matrix without phase shifter," *IEEE Microwave and Wireless Components Letters*, vol. 24, no. 5, pp. 306–308, 2014.

[11] S. A. Babale, S. K. Abdul Rahim, O. A. Barro, M. Himdi, and M. Khalily, "Single layered 4×4 butler matrix without phase-shifters and crossovers," *IEEE Access*, vol. 6, pp. 77289–77298, 2018.

[12] H. Ren, B. Arigong, M. Zhou, J. Ding, and H. Zhang, "A novel design of 4×4 Butler matrix with relatively flexible phase differences," *IEEE Antennas and Wireless Propagation Letters*, vol. 15, pp. 1277–1280, 2016.

[13] Y. Wu, J. Shen, and Y. Liu, "Comments on "quasi-arbitrary phase-difference hybrid coupler"," *IEEE Transactions on Microwave Theory and Techniques*, vol. 61, no. 4, pp. 1725–1727, 2013.

[14] T. K. Sarkar, Z. A. Maricevic, J. B. Zhang, and A. R. Djordjevic, "Evaluation of excess inductance and capacitance of microstrip junctions," *IEEE Transactions on Microwave Theory and Techniques*, vol. 42, no. 6, pp. 1095–1097, 1994.